Supplementary Data

Materials and Methods

RNA extraction and reverse transcriptase–polymerase chain reaction analysis

For total RNA extraction, gravid hermaphrodites were washed off the plates with M9 buffer and dissolved in 5 *M* NaOH bleaching solution. Embryos were collected and washed several times with M9 buffer. RNA was extracted from embryos using the NucleoSpin RNA II (Macherey-Nagel) kit following the manufacturer's instructions. The total RNA was DNase-treated using the Amplification Grade DNase I (Sigma) and 1 μg of DNase-treated RNA was reverse transcribed in a 20 μL reaction mixture. cDNA was generated using the iScript™ cDNA Synthesis Kit (Biorad). One microgram of cDNA was used for nested reverse transcriptase–polymerase chain reactions (RT-PCRs) using MBL-Taq DNA Polimerase (Dominion-MBL) with the following primers:

trx-2 wt *and* tm2720 alleles
5′- ATGACACAATTACGTCATTTTTC -3′ (forward)
5′- CTGTTTTCGACATTGATTCTGTT -3′ (forward)
5′- ACTTCCTTGTCTTCCGTTTAC -3′ (reverse)

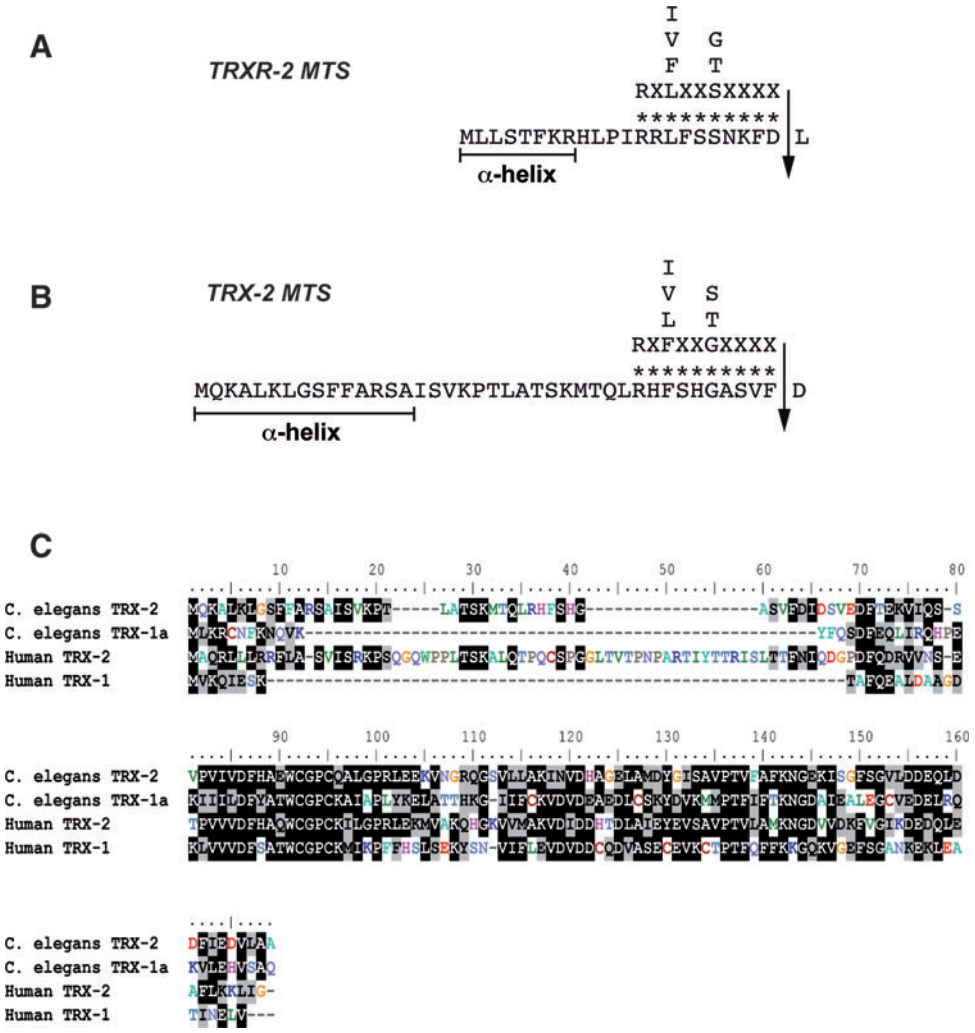

SUPPLEMENTARY FIG. S1. TRXR-2 and TRX-2 mitochondrial targeting sequences (MTS) and amino acid alignment of *C. elegans* TRX-2. (A, B) MTS of TRXR-2 and TRX-2, predicted by the PSORT algorithm (http://psort.hgc.jp/). The *arrow* indicates the predicted final mitochondrial peptide protease cleavage site determined by the consensus motif of the two protease models shown above the sequence, where X means any amino acid residue (8). **(C)** Alignment of the amino acid sequence of *C. elegans* TRX-2 with that of *C. elegans* TRX-1a (22), human TRX-1 (28) and human TRX-2 (4). Identical residues are shown in *black boxes*, while similar residues are shown in *gray*. The Megalign software integrated in the Lasergene Suite package (DNASTAR) was used for alignment of the sequences by the Clustal W method (26). TRX, thioredoxin; TRXR, thioredoxin reductase.

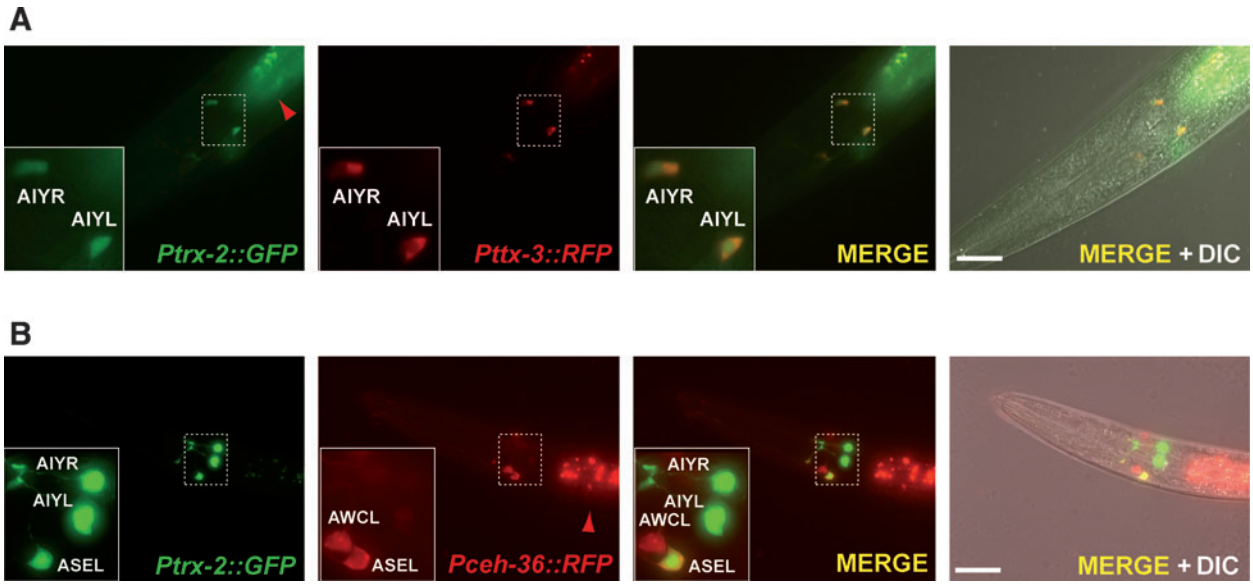

SUPPLEMENTARY FIG. S2. TRX-2 is expressed in ASEL and AIYL/R neurons. Transgenic animals expressing simultaneously the transcriptional fusions *Pttx-3::RFP* (27) or *Pceh-36::RFP* (10) along with *Ptrx-2::GFP* demonstrate colocalization by the merged yellow color in AIYL/R neurons **(A)** or ASEL neurons **(B)**, respectively. Note that RFP has a much weaker signal in the nucleus, resulting in a green nucleus surrounded by a yellowish cytoplasm in the merged images. *Red arrowheads* denote the intestinal autofluorescent granules. *Insets* show amplification of the respective dashed areas. Image analysis was performed as described in the Materials and Methods section. Bar 20 μm. RFP, red fluorescent protein; TRX, thioredoxin; TRXR, thioredoxin reductase.

trxr-2 wt and tm2047 alleles
5′- TCAATTACTTCAATGCCTATGCCG -3′ (forward)
5′- CAAGATTGTGATAACTGGTACAGAC -3′ (forward)
5′- TTATCCACAGCATCCCTGAGTTC -3′ (reverse)

trxr-2 ok2267 allele
5′- CAATTTTCTGATGCTTCTATC -3′ (forward)
5′- GTAATTGGAGCAGGATCTGGAG -3′ (forward)
5′- CTGCGGCATTTGGTCCAACA -3′ (reverse)
5′- TTATCCACAGCATCCCTGAGTTC -3′ (reverse)

ama-1 wt allele
5′- TTCCAAGCGCCGCTGCGCATTGTC -3′ (forward)
5′- CAGAATTTCCAGCACTCGAGGAGCGGA -3′ (reverse)

Recombinant protein expression and purification

trx-2 cDNA from N2 wild-type and *trx-2 (tm2720)* mutant (see RNA extraction and RT-PCR analysis section, Supplementary Materials and Methods) was amplified with the forward primer 5′- CATGCATATGGACATTGATTCTG TTGAAG-3′ and the reverse primer 5′- CGACGGATCCCT ACTAATTTAAATGAACCATTAAACT-3′ and cloned into the *Nde*I and *Bam*HI restrictions sites of the pET-15b vector (Novagen) to generate the constructs pET-15b::His-CeTRX-2 and pET-15b::His-CeΔTRX-2, respectively. These constructs were used to transform the *Escherichia coli* BL21 (DE3) strain and recombinant protein expression was induced at 37°C and 200 rpm during 4 h by adding 1 m*M* IPTG to a cell culture of 0.5–0.7 optical density in a 100 mL LB medium supplemented with 0.1 mg/mL ampicillin. Cells were collected by centrifugation, immediately resuspended in 5 mL of Tris-HCl 20 m*M* pH 8.0, NaCl 100 m*M*, DNaseI 60 μg, lysozime 3 mg and β-mercaptoethanol 5 m*M* and incubated for 15 min at room temperature with gentle shaking. Next, the preparation was sonicated for 5 min on ice and the cell-free extract was obtained by centrifugation at 12,000 × *g* during 30 min at 4°C. Recombinant His-CeTRX-2 and His-CeΔTRX-2 proteins were purified from the cell-free extract using a BD TALON® Metal Affinity column (Clontech) equilibrated with Tris-HCl 20 m*M* pH 8.0, NaCl 100 m*M* and eluted with imidazole 25 m*M*. Finally, the purified protein was dialyzed against sodium phosphate buffer 20 m*M* pH 7.4 to remove imidazole from the preparation.

Thioredoxin activity assays

For the 1,4-dithio-D-threitol (DTT) assay, 25 μL of a reaction mix (composed of 40 μL Tris-HCl 1 *M* pH 7.5, 10 μL ethylenediaminetetraacetic acid (EDTA) 0.2 *M* and 200 μL of bovine insulin 10 mg/mL) were mixed with the protein preparation in a final assay volume of 200 μL. The reaction was initiated by adding 2 μL of DTT 100 m*M* and the thioredoxin activity was measured by monitoring the increase of absorbance at 595 nm due to free-B chain precipitation over time.

For the reduced nicotinamide adenine dinucleotide phosphate (NADPH) and thioredoxin reductase assay, 20 μL of a reaction mix (composed of 40 μL HEPES 1 *M* pH 7.4, 8 μL EDTA 0.2 *M*, 8 μL NADPH 40 mg/mL and 100 μL insulin 10 mg/mL) were mixed with the protein preparation in a final assay volume of 200 μL. The reaction was initiated by adding 1 μL rat TrxR1 1.5 mg/mL and the thioredoxin activity was measured by monitoring the decrease of absorbance at 340 nm due to NADPH consumption over time.

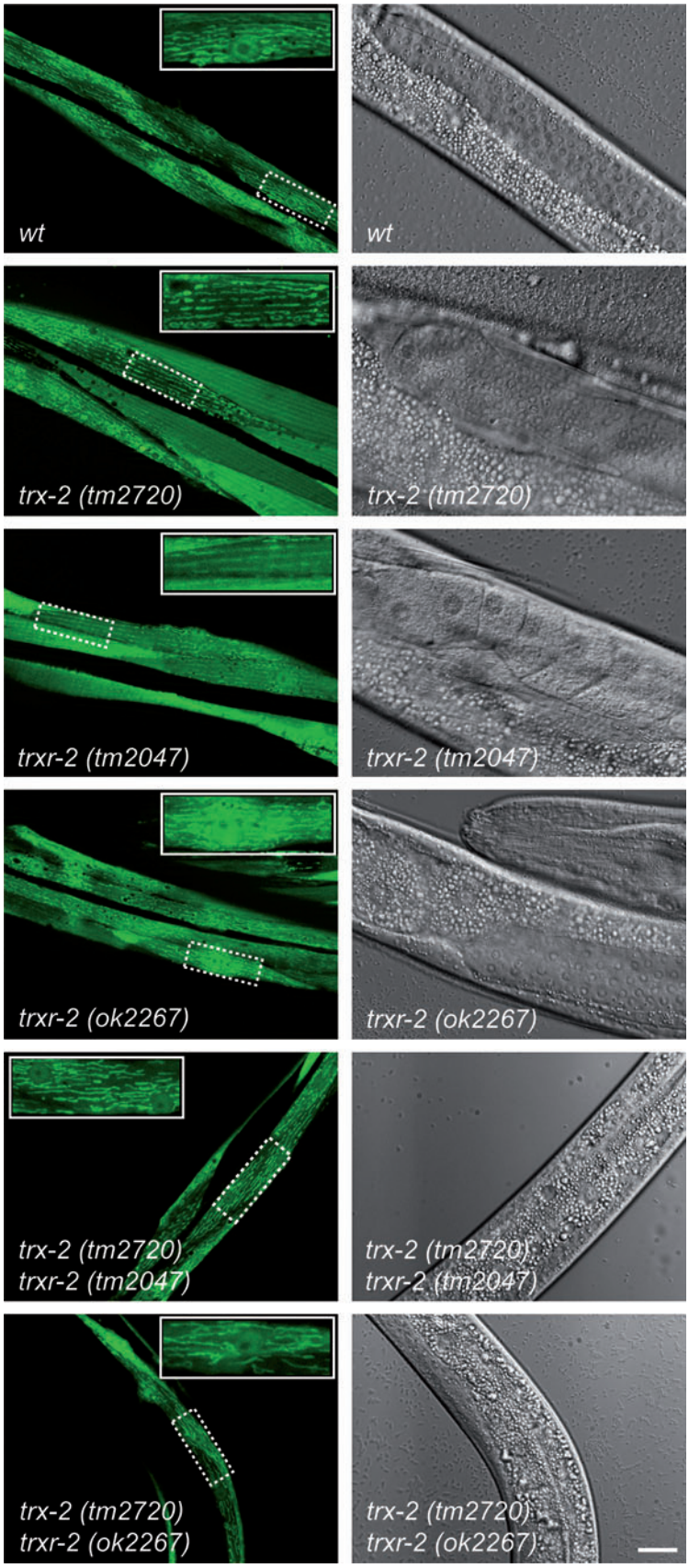

SUPPLEMENTARY FIG. S3. Mitochondrial morphology of *trx-2* and *trxr-2* mutants. Wild-type, *trx-2* and *trxr-2* single and double mutant strains expressing the construct *Pmyo-3::MTS::GFP* (12) were examined for mitochondria morphology in body wall muscle cells. *Left panels* show fluorescence optics and *right panels* DIC optics. The typical tubular morphology of muscle cells mitochondria is maintained in all strains examined regardless of the genetic background. *Insets* show amplification of the respective dashed areas. Image analysis was performed as described in the Materials and Methods section. Bar 20 μm. DIC, differential interference contrast.

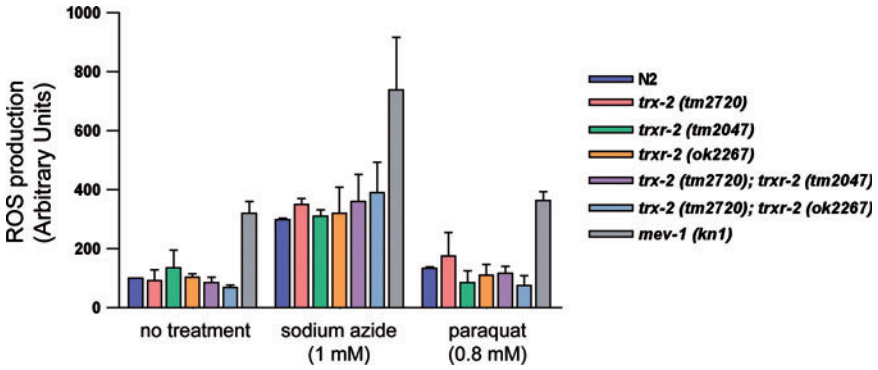

SUPPLEMENTARY FIG. S4. Reactive oxygen species (ROS) production by the mitochondrial thioredoxin system mutants. ROS production was carried out using the membrane-permeable nonfluorescent dye H2-DCF-DA. Upon entry into the cell, H2-DCF-DA is deacetylated to H2-DCF and becomes membrane impermeable. H2-DCF then reacts with ROS and oxidizes to DCF, which is a fluorescent compound. Synchronized L4 animals were used and the fluorescence was determined after 5 h treatment at 20°C. The graph shows the average of three independent experiments and the error bars represent the standard error of the mean. Two-way analysis of variance test was performed and differences were found to be not significant in all cases ($p > 0.05$), except for *mev-1 (kn1)* mutant ($p < 0.001$), which was used as a positive control due to its high rate of ROS production (9). H2-DCF-DA, 2,7-dichlorodihydrofluorescein-diacetate.

Green fluorescent protein expression constructs and transgenesis

All constructs were used at 50 ng/μL (except for pVZ25 [*Punc-32::GFP*] at 10 ng/μL) along with the pRF4 plasmid that carries the *rol-6*(*su1006*) dominant transformation marker (50 ng/μL) to generate stable transgenic lines by microinjection (21). At least two independent transgenic lines carrying nonintegrated arrays showing identical or very similar expression patterns were obtained for each construct (except for pVZ211 [*Punc-32::MTS::GFP*] construct with only one line).

Stress assays

In all cases, animals that did not show pharyngeal pumping or movement after mechanical stimulation were scored as dead and removed from the assay plates.

Sodium arsenite treatment. Thirty L4 hermaphrodites were transferred onto seeded NGM plates containing 10 m*M* sodium arsenite (Sigma) and scored every hour for survival (23).

Juglone treatment. Thirty young adult gravid hermaphrodites were placed onto freshly made seeded NGM plates

SUPPLEMENTARY FIG. S5. Demonstration of effective *trx-2* and *trxr-2* RNAi downregulation, total Aβ content of constitutive and inducible Aβ strains, Aβ-dependent paralysis and TRXR-2 overproduction levels. (A) Transgenic worms expressing the constructs *Ptrx-2::trx-2::GFP* and *Punc-32::trxr-2::GFP* were subjected to two generations of RNAi feeding in HT-115 bacteria expressing no dsRNA, *trx-2* or *trxr-2* dsRNA, respectively. All micrographs using the same transgene were taken with identical image capture settings and adjustment of brightness and contrast, when needed, was done identically for all images from the same transgene. Note that both *trx-2* and *trxr-2* RNAi treatments efficiently and specifically downregulate their corresponding transgenes, thus validating the RNAi approach. Image analysis was performed as described in the Materials and Methods section. Bar 200 μm. **(B)** Aβ immunoblot with 6E10 monoclonal antibody of CL2006 and CL2750 constitutive Aβ strains. All *lanes* were loaded with total protein extract from 100 one-day adult synchronized worms grown on OP50 bacteria. Note that the CL2006 strain has a slight higher Aβ content as compared with the CL2750 strain. α-tubulin is used as loading control. One blot is shown out of two independent trials with similar results. The quantification of the blots and the statistical analyses are included in Supplementary Figure S6B. **(C)** Progressive paralysis of Aβ inducible CL4176, *smg-1 (cc546); dvIs27 [Pmyo-3::Aβ3–42::let-858 3′-UTR; rol-6 (su1006)]* worms growing on HT-115 bacteria expressing either no dsRNA (■), *trx-2* dsRNA (▲), or *trxr-2* dsRNA (●). The graph shows one representative experiment out of two independent trials with similar results. Aβ production was induced on a 23°C upshift. **(D)** Progressive paralysis of CL4176 worms and its derivative transgenic strain VZ297 carrying the extrachromosomal array *vzEx111 [Pmyo-3::trxr-2::trxr-2 3′-UTR; Punc-122::GFP]* growing on HT-115 bacteria expressing either no dsRNA (■, □) or *trxr-2* dsRNA (●, ○). The graph shows one representative experiment out of two independent trials with similar results. Aβ production was induced upon a 25°C upshift. **(E)** Aβ immunoblot with 6E10 monoclonal antibody of CL4176 and VZ297 Aβ inducible strains. All *lanes* were loaded with total protein extract from 100 worms after 24 h Aβ production induced upon a 25°C upshift. Animals were grown on HT-115 bacteria expressing either no dsRNA or *trxr-2* dsRNA. Note the clear decrease in Aβ content found in TRXR-2 overexpressing animals, an effect that is abolished when *trxr-2* overexpression is downregulated by RNAi. One blot is shown out of two independent trials with similar results. The quantification of the blots and the statistical analyses are included in Supplementary Figure S6C. **(F)** TRXR-2 immunoblot of CL2006 and CL4176 Aβ strains and their respective TRXR-2 overexpressing derivatives VZ209 and VZ297. All *lanes* were loaded with total protein extract from 100 synchronized 1-day adult worms grown on OP50 bacteria. α-tubulin was used as loading control. The TRXR-2 levels (monomer and dimer) were compared between the two independent TRXR-2 overexpressing strains and their respective nontransgenic siblings within the same blot. One blot is shown out of two independent trials with similar results. The quantification of the blots and the statistical analyses are included in Supplementary Figure S6D.

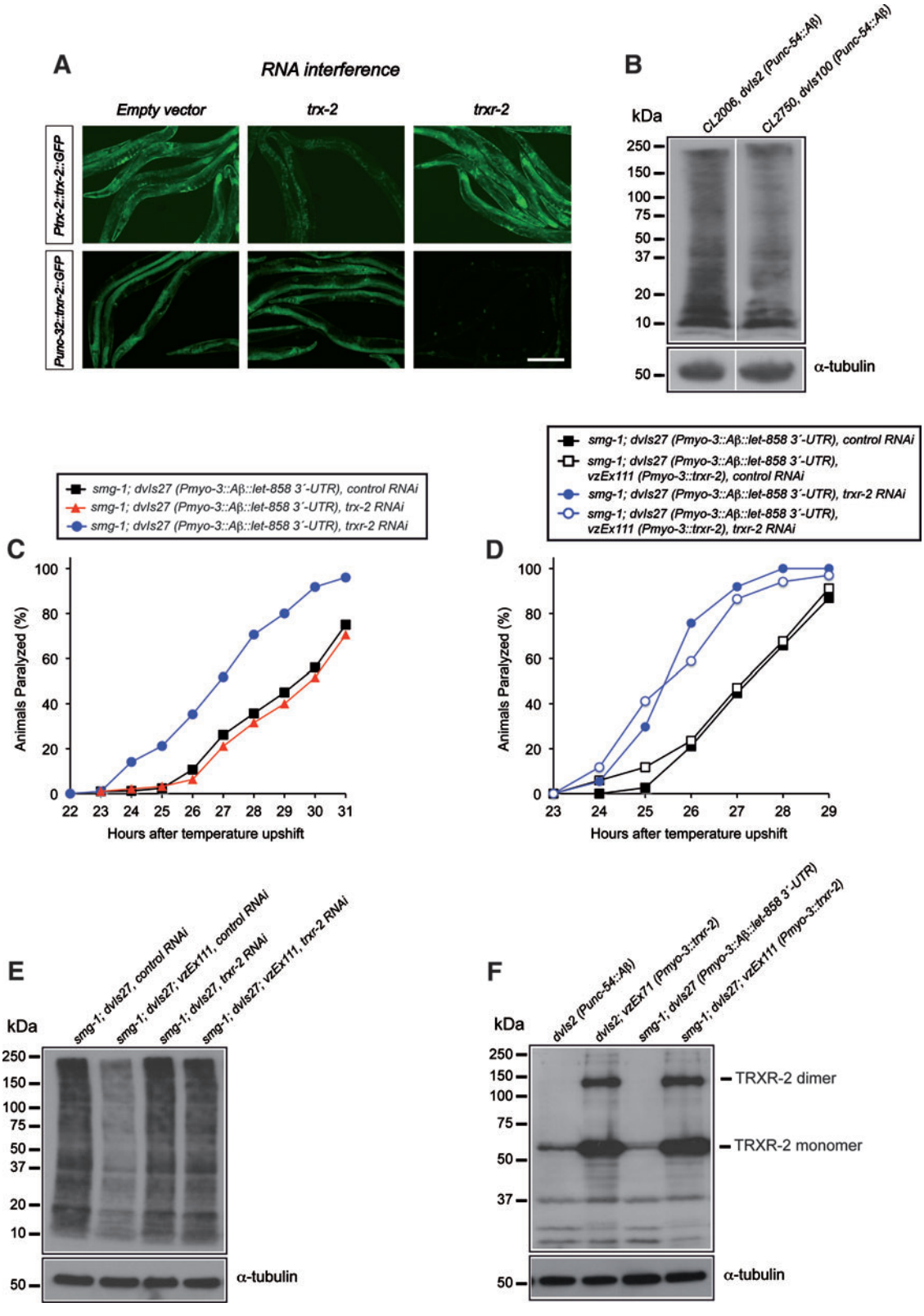
A
RNA interference
Empty vector
trx-2
trxr-2
Ptrx-2::trx-2::GFP
Punc-32::trxr-2::GFP
B
CL2006, dvIs2 (Punc-54::Aβ)
CL2750, dvIs100 (Punc-54::Aβ)
kDa
250
150
100
75
50
37
20
10
50
α-tubulin
C
smg-1; dvIs27 (Pmyo-3::Aβ::let-858 3′-UTR), control RNAi
smg-1; dvIs27 (Pmyo-3::Aβ::let-858 3′-UTR), trx-2 RNAi
smg-1; dvIs27 (Pmyo-3::Aβ::let-858 3′-UTR), trxr-2 RNAi
Animals Paralyzed (%)
Hours after temperature upshift
D
smg-1; dvIs27 (Pmyo-3::Aβ::let-858 3′-UTR), control RNAi
smg-1; dvIs27 (Pmyo-3::Aβ::let-858 3′-UTR), vzEx111 (Pmyo-3::trxr-2), control RNAi
smg-1; dvIs27 (Pmyo-3::Aβ::let-858 3′-UTR), trxr-2 RNAi
smg-1; dvIs27 (Pmyo-3::Aβ::let-858 3′-UTR), vzEx111 (Pmyo-3::trxr-2), trxr-2 RNAi
Animals Paralyzed (%)
Hours after temperature upshift
E
kDa
smg-1; dvIs27, control RNAi
smg-1; dvIs27; vzEx111, control RNAi
smg-1; dvIs27, trxr-2 RNAi
smg-1; dvIs27; vzEx111, trxr-2 RNAi
α-tubulin
F
kDa
dvIs2 (Punc-54::Aβ)
dvIs2; vzEx71 (Pmyo-3::trxr-2)
smg-1; dvIs27 (Pmyo-3::Aβ::let-858 3′-UTR)
smg-1; dvIs27; vzEx111 (Pmyo-3::trxr-2)
TRXR-2 dimer
TRXR-2 monomer
α-tubulin

A *Quantitative data and statistical analysis of Aβ levels from FIG. 8D immunoblots. (3 independent trials)*

	dvIs2 (Punc-54::Aβ)		*dvIs2 (Punc-54::Aβ); vzEx71 (Pmyo-3::trxr-2)*	
	control RNAi	*trxr-2 RNAi*	*control RNAi*	*trxr-2 RNAi*
Blot #1 (Aβ / α-tubulin)	3.415716339	4.285781992	0.563505154	2.473328978
Blot #2 (Aβ / α-tubulin)	3.339312579	2.512843944	0.764199873	3.537525987
Blot #3 (Aβ / α-tubulin)	3.222903689	3.763625592	0.661562156	3.070106684
Mean Aβ content	3.325977536	3.520750509	0.663089061	3.026987216
Relative to dvIs2 control RNAi	1	1.058561121	0.199366669	0.910104528
Standard deviation	0.097095556	0.911080984	0.100356072	0.533407241
Statistics (unpaired two-tailed t-test)		0.365691984	2.50517E-06	0.196790869

B *Quantitative data and statistical analysis of Aβ levels from Supplemental FIG. 5B immunoblots. (2 independent trials)*

	CL2006 dvIs2 (Punc-54::Aβ)	*CL2750 dvIs27 (Pmyo-3::Aβ)*
Blot #1 (Aβ / α-tubulin)	1.231867876	0.825153482
Blot #2 (Aβ / α-tubulin)	1.172368869	0.828367294
Mean Aβ content	1.202118373	0.826760388
Relative to CL2006	1	0.687752892
Standard deviation	0.04207215	0.002272511
Statistics (unpaired two-tailed t-test)		0.049739398

C *Quantitative data and statistical analysis of Aβ levels from Supplemental FIG. 5E immunoblots. (2 independent trials)*

	smg-1 (cc546); dvIs27 (Pmyo-3::Aβ)		*smg-1 (cc546); dvIs27 (Pmyo-3::Aβ) vzEx111 (Pmyo-3::trxr-2)*	
	control RNAi	*trxr-2 RNAi*	*control RNAi*	*trxr-2 RNAi*
Blot #1 (Aβ / α-tubulin)	3.476665069	3.286848341	1.402164948	2.436207272
Blot #2 (Aβ / α-tubulin)	2.683948617	3.178495279	1.593168881	3.420893971
Mean Aβ content	3.080306843	3.232671811	1.497666915	2.928550621
Relative to smg-1; dvIs27 control RNAi	1	1.049464218	0.486207051	0.905922652
Standard deviation	0.560535179	0.076617185	0.135060176	0.696278642
Statistics (unpaired two-tailed t-test)		0.369974739	0.001990501	0.300877017

D *Quantitative data and statistical analysis of TRXR-2 levels from Supplemental FIG. 5F immunoblot. (2 trials with two independent TRXR-2 overexpressing strains)*

	dvIs2 (Punc-54::Aβ)		*smg-1 (cc546); dvIs27 (Pmyo-3::Aβ)*	
	non transgenic control sibling	*vzEx71 (Pmyo-3::trxr-2)*	*non transgenic control sibling*	*vzEx111 (Pmyo-3::trxr-2)*
Blot #1 (TRXR-2 / α-tubulin)	1.1860587	5.161625008	2.057082856	9.869099564
Blot #2 (TRXR-2 / α-tubulin)	1.037731517	6.980635335	1.775925261	5.307878137
Mean TRXR-2 content	1.111895109	6.071130172	1.916504058	7.58848885
Relative to non transgenic control	1	5.460164475	1	3.959547499
Standard deviation	0.104883157	1.286234537	0.198808442	3.225270601
Statistics (unpaired two-tailed t-test)		0.016114957		0.06555736

SUPPLEMENTARY FIG. S6. Quantification and statistical analyses of Aβ and TRXR-2 western blots. The quantification of the blots was performed with the ImageJ Software and the statistical analysis was implemented using the Microsoft Excel Software.

Supplementary Table S1. Strains Used in This Study

Strain name	*Genotype*	*Reference/source*
Basic strains		
N2	Wild type, DR subclone of CB original (Tc1 pattern I)	CGC[a]
VZ13	*trx-2 (tm2720) V*	This study
VZ12	*trxr-2 (tm2047) III*	This study
VZ15	*trxr-2 (ok2267) III*	This study
VZ17	*trxr-2 (tm2047) III; trx-2 (tm2720) V*	This study
VZ22	*trxr-2 (ok2267) III; trx-2 (tm2720) V*	This study
rrf-3 strains		
NL2099	*rrf-3 (pk1426) II*	(25)
VZ29	*rrf-3 (pk1426) II; trx-2 (tm2720) V*	This study
VZ30	*rrf-3 (pk1426) II; trxr-2 (tm2047) III*	This study
VZ31	*rrf-3 (pk1426) II; trxr-2 (ok2267) III*	This study
VZ33	*rrf-3 (pk1426) II; trxr-2 (tm2047) III; trx-2 (tm2720) V*	This study
VZ38	*rrf-3 (pk1426) II; trxr-2 (ok2267) III; trx-2 (tm2720) V*	This study
daf-16::GFP strains		
TJ356	*zIs356 [Pdaf-16::daf-16::GFP; pRF4 (rol-6 (su1006))] IV*	(7)
VZ25	*zIs356 [Pdaf-16::daf-16::GFP; pRF4 (rol-6 (su1006))] IV; trx-2 (tm2720) V*	This study
VZ23	*trxr-2 (tm2047) III; zIs356 [Pdaf-16::daf-16::GFP; pRF4 (rol-6 (su1006))] IV*	This study
VZ24	*trxr-2 (ok2267) III; zIs356 [Pdaf-16::daf-16::GFP; pRF4 (rol-6 (su1006))] IV*	This study
skn-1::GFP strains		
LD001	*Is007 [Pskn-1::skn-1::GFP; pRF4 (rol-6 (su1006))] X*	(1)
VZ26	*trx-2 (tm2720) V; Is007 [Pskn-1::skn-1::GFP; pRF4 (rol-6 (su1006))] X*	This study
VZ39	*trxr-2 (tm2047) III; Is007 [Pskn-1::skn-1::GFP; pRF4 (rol-6 (su1006))] X*	This study
VZ40	*trxr-2 (ok2267) III; Is007 [Pskn-1::skn-1::GFP; pRF4 (rol-6 (su1006))] X*	This study
Other stress reporter strains		
TK22	*mev-1 (kn1) III*	(9)
GA480	*sod-2 (gk257) I; sod-3 (tm760) X*	(6)
SJ4005	*zcIs4 [Phsp-4::GFP] V*	(3)
SJ4100	*zcIs13 [Phsp-6::GFP] V*	(29)
CL2070	*dvIs70 [pCL25 (Phsp-16.2::GFP); pRF4 (rol-6 (su1006))]*	(16)
CF1553	*muIs84 [pAD76 (Psod-3::GFP)]*	(13)
CL2166	*dvIs19 [pAF15 (Pgst-4::GFP::NLS); pRF4 (rol-6 (su1006))]*	(17)
trxr-1; trxr-2 strains		
VZ14	*trxr-2 (tm2047) III; trxr-1 (sv47) IV*	This study
VZ21	*trxr-2 (ok2267) III; trxr-1 (sv47) IV*	This study
daf-2 and daf-16 strains		
CB1370	*daf-2 (e1370) III*	(11)
VZ87	*daf-2 (e1370) III; trx-2 (tm2720) V*	This study
VZ89	*daf-2 (e1370) III; trxr-2 (tm2047) III*	This study
VZ90	*daf-2 (e1370) III; trxr-2 (ok2267) III*	This study
CF1038	*daf-16 (mu86) I*	(14)
VZ102	*daf-16 (mu86) I; trx-2 (tm2720) V*	This study
VZ103	*daf-16 (mu86) I; trxr-2 (tm2047) III*	This study
VZ101	*daf-16 (mu86) I; trxr-2 (ok2267) III*	This study
GM6	*fer-15 (b26) II; daf-2 (e1370) III*	Manuel Muñoz gift
VZ117	*fer-15 (b26) II; daf-2 (e1370) III; trx-2 (tm2720) V*	This study
VZ129	*fer-15 (b26) II; daf-2 (e1370) III; trxr-2 (tm2047) III*	This study
VZ116	*fer-15 (b26) II; daf-2 (e1370) III; trxr-2 (ok2267) III*	This study
trx-2 and trxr-2 GFP fusion strains		
VZ74	*vzEx18 [pVZ239 (Ptrx-2::GFP); pRF4 (rol-6 (su1006))]*	This study
VZ55	*vzEx8 [pVZ202 (Ptrx-2::trx-2::GFP); pRF4 (rol-6 (su1006))]*	This study
VZ83	*vzEx21 [pVZ25 (Punc-32::GFP); pRF4 (rol-6 (su1006))]*	This study
VZ42[b]	*vzEx1 [pVZ212 (Punc-32::trxr-2::GFP); pRF4 (rol-6 (su1006))]*	This study
VZ62	*vzEx12 [pVZ234 (Ptrxr-2::GFP); pRF4 (rol-6 (su1006))]*	This study
VZ69	*vzEx14 [pVZ222 (Ptrxr-2::trxr-2::GFP); pRF4 (rol-6 (su1006))]*	This study
Mitochondrial morphology strains		
VZ104	*vzEx23 [pVZ228 (Pmyo-3::MTS::GFP); pRF4 (rol-6 (su1006))]*	This study[c]
VZ121	*trx-2 (tm2720) V; vzEx23 [pVZ228 (Pmyo-3::MTS::GFP); pRF4 (rol-6 (su1006))]*	This study

(*continued*)

Table S1. (Continued)

Strain name	*Genotype*	*Reference/source*
VZ122	*trxr-2 (tm2047) III; vzEx23 [pVZ228 (Pmyo-3::MTS::GFP); pRF4 (rol-6 (su1006))]*	This study
VZ125	*trxr-2 (ok2267) III; vzEx23 [pVZ228 (Pmyo-3::MTS::GFP); pRF4 (rol-6 (su1006))]*	This study
VZ110	*trxr-2 (tm2047) III; trx-2 (tm2720) V; vzEx27 [pVZ228 (Pmyo-3::MTS::GFP); pRF4 (rol-6 (su1006))]*	This study
VZ111	*trxr-2 (ok2267) III; trx-2 (tm2720) V; vzEx28 [pVZ228 (Pmyo-3::MTS::GFP); pRF4 (rol-6 (su1006))]*	This study
Mitochondrial colocalization strains		
PS6187	*unc-119 (ed3) III; syEx1155 [pAM34.1 (Pmyo-3::TOM20::mRFP::3xMyc); unc-119(+)]*	Amir Sapir and Paul Sternberg gift
VZ141	*vzEx8 [pVZ202 (Ptrx-2::trx-2::GFP); pRF4 (rol-6 (su1006))]; syEx1155 [pAM34.1 (Pmyo-3::TOM20::mRFP::3xMyc); unc-119(+)]*	This study
VZ142	*vzEx1 [pVZ212 (Punc-32::trxr-2::GFP); pRF4 (rol-6 (su1006))]; syEx1155 [pAM34.1 (Pmyo-3::TOM20::mRFP::3xMyc); unc-119(+)]*	This study
AIY colocalization strains		
OH1098	*otIs133 [Pttx-3::RFP; unc-4(+)]*	(27)
VZ167	*otIs133 [Pttx-3::RFP; unc-4(+)]; vzEx18 [pVZ239 (Ptrx-2::GFP); pRF4 (rol-6 (su1006))]*	This study
ASE colocalization strains		
OH4165	*otIs151 [Pceh-36::RFP; pRF4 (rol-6 (su1006))]; otEx2416 [Pgcy-21::GFP; Punc-122::GFP]*	(24)
VZ179	*otIs151 [Pceh-36::RFP; pRF4 (rol-6 (su1006))]; otEx2416 [Pgcy-21::GFP; Punc-122::GFP]; vzEx18 [pVZ239 (Ptrx-2::GFP); pRF4 (rol-6 (su1006))]*	This study
*A*β-peptide *strains*		
CL2006	*dvIs2 [pCL12 (Punc-54::Aβ 3–42::unc-54 3′-UTR); pRF4 (rol-6 (su1006))] II*	(15)
VZ18	*dvIs2 [pCL12 (Punc-54::Aβ 3–42::unc-54 3′-UTR); pRF4 (rol-6 (su1006))] II; trx-2 (tm2720) V*	This study
CL2750	*dvIs100 [pCL354 (Punc-54::Aβ 1–42::unc-54 3′-UTR); pCL26 (Pmtl-2::GFP)]*	C.D. Link, unpublished data
VZ223	*trxr-2 (tm2047) III; dvIs100 [pCL354 (Punc-54::Aβ 1–42::unc-54 3′-UTR); pCL26 (Pmtl-2::GFP)]*	This study
VZ209	*dvIs2 [pCL12 (Punc-54::Aβ 3–42::unc-54 3′-UTR); pRF4 (rol-6 (su1006))] II; vzEx71 [pVZ394 (Pmyo-3::trxr-2::trxr-2 3′-UTR); Punc-122::GFP]*	This study
CL4176	*smg-1 (cc546ts) I; dvIs27 [pAF29 (Pmyo-3::Aβ 3–42::let-858 3′-UTR); pRF4 (rol-6 (su1006))] X*	(20)
VZ297	*smg-1 (cc546ts) I; dvIs27 [pAF29 (Pmyo-3::Aβ 3–42::let-858 3′-UTR); pRF4 (rol-6 (su1006))] X; vzEx111 [pVZ394 (Pmyo-3::trxr-2::trxr-2 3′-UTR); Punc-122::GFP]*	This study

[a]Caenorhabditis Genetics Center (www.cbs.umn.edu/CGC/).
[b]MTS of *trxr-2* gene.
[c]The *Pmyo-3::MTS::GFP* construct was described in Labrousse *et al.* (12).
MTS, mitochondrial targeting sequence; GFP, green fluorescent protein.

containing 240 μM juglone (Sigma) and viability was determined every 2 h during a total period of 8 h (5).

Paraquat treatment. One hundred L4 hermaphrodites were placed onto seeded NGM plates containing 4 m*M* paraquat (Sigma). Survival was monitored every 24 h.

Sodium azide treatment. Thirty L4 hermaphrodites were placed onto seeded NGM plates supplemented with 1 m*M* sodium azide (Sigma) for 18 h at 20°C. The animals were then transferred to seeded NGM plates without sodium azide and scored for survival after a 3-h recovery period (2).

Heat-shock treatment. Thirty L4 hermaphrodites were placed on prewarmed (37°C) seeded NGM plates and incubated at 37°C. Survival was monitored every hour.

Microsoft Excel Program was used for graphical display and statistical analysis was performed with GraphPad Prism software package (GraphPad Software).

Reactive oxygen species determination

Reactive oxygen species formation was quantified using the membrane-permeable nonfluorescent dye 2,7-dichlorodihydrofluorescein-diacetate (H2-DCF-DA; Sigma) as previously described by (2). Synchronized L4 hermaphrodites were placed on NGM plates (control) and NGM plates with 1 m*M* sodium azide or 0.8 m*M* paraquat and incubated at 20°C for 5 h. Next, the animals were washed off the plates with M9 buffer to reduce bacterial content and a 50 μL volume of worm suspension was pipetted in four replicates into the wells of a 96-well plate with opaque walls and bottom and

Supplementary Table S2. Brood Sizes of the trx-2 and trxr-2 Mutants

Strain name	*Genotype*	*Average brood size*[a] ± *SD*
N2	Wild type	255 ± 57
VZ13	*trx-2 (tm2720) V*	305 ± 61[b]
VZ12	*trxr-2 (tm2047) III*	285 ± 41
VZ15	*trxr-2 (ok2267) III*	251 ± 54
VZ17	*trxr-2 (tm2047) III; trx-2 (tm2720) V*	300 ± 53
VZ22	*trxr-2 (ok2267) III; trx-2 (tm2720) V*	219 ± 62

[a]The total number of progeny from 10 worms of each genotype were determined.
[b]$p < 0.05$ by unpaired two-tailed *t*-test.
SD, standard deviation.

allowed to equilibrate to room temperature. Fifty micro liters of a fresh 100 μM H2-DCF-DA solution was pipetted to the suspensions, resulting in a final concentration of 50 μM. On each plate, control wells containing nematodes from each treatment without H2-DCF-DA and wells containing H2-DCF-DA without animals were prepared in parallel. Immediately after addition of H2-DCF-DA, basal fluorescence was measured in a microplate reader (PolarStar Omega. BMG, LabTech) at excitation/emission wavelengths of 485 and 520 nm, respectively. Plates were kept for 1 h shaking at 20°C. Then, a second measurement was performed. The initial fluorescence and the fluorescence signals of control wells were subtracted from the second measurement. Values were normalized to protein content, which was determined using the bicinchoninic acid protein assay kit (Pierce). We used the GraphPad Prism software package (GraphPad Software) for graphical display and statistical analysis.

Supplementary Table S3. Genes Tested in RNA Interference Feeding Assays for Synthetic Defects with Mutants of the Mitochondrial Thioredoxin System

Gene category	*Gene name*	*Gene sequence designation*	*Synthetic phenotype*
Thioredoxins	*trx-1*	B0228.5	No
	trx-2	B0024.9	No
	trx-3	M01H9.1	No
	txl	Y54E10A.3	No
	dnj-27	Y47H9C.5	No
	trx-4	Y44E3A.3	No
	trx-5	K02H11.6	No
Thioredoxin reductases	*trxr-1*	C06G3.7	No
	trxr-2	ZK637.10	No
Glutaredoxins	*glrx-5*	Y49E10.2	NA[a]
	glrx-10	Y34D9A.6	No
	glrx-21	ZK121.1	No
	glrx-22	C07G1.8	No
Peroxiredoxins	*prdx-2*	F09E5.15	NA[a]
	prdx-3	R07E5.2	No
	prdx-6	Y38C1AA.11	No
Glutathione reductase	*gsr-1*	C46F11.2	No

All genes were tested by conducting RNA interference feeding with the indicated gene in the following genetic backgrounds. The *rrf-3 (pk1426)* mutation increases the sensitivity to RNAi (25):
NL2099, *rrf-3 (pk1426) II*
VZ29, *rrf-3 (pk1426) II; trx-2 (tm2720) V*
VZ30, *rrf-3 (pk1426) II; trxr-2 (tm2047) III*
VZ31, *rrf-3 (pk1426) II; trxr-2 (ok2267) III*
VZ33, *rrf-3 (pk1426) II; trxr-2 (tm2047) III; trx-2 (tm2720) V*
VZ38, *rrf-3 (pk1426) II; trxr-2 (ok2267) III; trx-2 (tm2720) V*
[a]Not applicable. RNAi of these genes caused larval arrest/slow growth of the *rrf-3 (pk1426)* control strain.

RNA interference

HT115 *E. coli* strain transformed with either pL4440 empty vector or the respective test clones were grown in liquid LB medium containing 100 μg/mL ampicillin for 15 h at 37°C before seeding the RNA interference (RNAi) plates containing 1 m*M* IPTG. The plates were incubated for 2 days at 37°C to induce dsRNA. Phenotypes were scored at 20°C from the first generation onward by allowing the interfered gravid hermaphrodites to lay eggs during 2 h on fresh RNAi plates.

Longevity assays

Tightly synchronized embryos from bleached gravid adult hermaphrodites were allowed to develop through the L4 larval stage and then transferred to fresh NGM plates in groups of 25 worms per plate for a total of 100 individuals per experiment. The day the animals reached the L4 larval stage was used as $t = 0$. Nematodes were transferred to fresh plates daily until progeny production ceased and after that, they were transferred every second to the third day but monitored daily for dead animals. Nematodes that did not respond to gentle prodding and displayed no pharyngeal pumping were scored as dead. Animals that crawled off the plate or died due to internal hatching or extruded gonad were censored and incorporated as such into the data set. Each survival assay was repeated twice. We used the GraphPad Prism software package (GraphPad Software) for graphical display and statistical analysis.

Paralysis phenotype, Aβ immunodetection and amyloid deposits determination

Worms were scored as paralyzed if they failed to propagate a full sinusoidal contraction after prodding or if their heads were associated with a "halo" of ingested bacterial lawn, indicative of an inability to move to access food. In experiments measuring paralysis of transgenic strains carrying extrachromosomal arrays, sibling worms containing the transgene were identified by green fluorescent protein (GFP) fluorescence of the marker transgene included in the extrachromosomal array. Identification of transgenic and nontransgenic worms was performed after paralysis scoring to prevent observer bias.

For Aβ immunoblotting, 100 worms from each strain (grown for 2 generations in the corresponding RNAi bacteria or grown in OP50 for one generation) were manually collected at their first day of adulthood (for Aβ constitutive strains) or after 24 h temperature upshift (for Aβ inducible strains) in 15 μL of lysis buffer (NaCl 150 m*M*, NP-40 1% and Tris-HCl 50 m*M* pH 8). After three cycles of freeze thawing in liquid nitrogen, 3 μL of Laemmli buffer 5× were added and the mix was heated at 95°C for 10 min. Proteins were separated by sodium dodecyl sulphate-polyacrylamide gel electrophoresis (SDS-PAGE) using a 4%–20% gradient polyacrylamide gel (BioRad) and transferred to Immobilon-P PVDF membranes (Millipore). Blots were probed with anti-Aβ monoclonal 6E10

(Covance) at a 1:1000 dilution and with mouse anti-IgG (Sigma) at 1:10,000 as a secondary antibody. The ECL kit (GE) was used for signal detection, following the manufacturer's instructions. Monoclonal anti-α-tubulin (Sigma) 1:10,000 was used as loading control. The quantification of Aβ blots was performed using the ImageJ Software and the statistical analysis was performed with the Microsoft Excel Software.

For Aβ immunohistochemistry, worms were fixed and permeabilized as previously described (19), except that glutaraldehyde was eliminated from the fixation step. Permeabilized worms were stained with monoclonal antibody 6E10 (Covance) at a final concentration of 5 mg/mL and with Alexa-labeled goat-anti-mouse secondary antibody (Invitrogen) at 20 mg/mL. Stained worms were imaged by shortwave epifluorescence microscopy using a Zeiss Axiophot microscope equipped with digital deconvolution capacity (Intelligent Imaging Innovations). Final images were assembled in Photoshop by projection images generated from a digital deconvolution series consisting of sixteen 1 μm optical sections.

For amyloid deposits staining, worms were stained with the amyloid-specific dye X-34 as previously described (18). Briefly, worms were propagated at 20°C and first-day adults were incubated for 2 h in 20 μL drops of 1 m*M* X-34 in 10 m*M* TRIS pH 7.5. Worms were then destained by rinsing once in a drop of phosphate-buffered saline and then transferring to NGM plates seeded with *E. coli* strain OP50 for overnight recovery at 20°C. Stained worms were anesthetized with sodium azide and imaged with a Zeiss Axiophot epifluorescence microscope as just described. The statistical analysis was performed with the Microsoft Excel Software.

Thioredoxin reductase 2 antibody production and immunodetection

The synthetic peptides Ac-RTDKRSGKILADEFDRASC-amide and Ac-CVKLHITKRSGQDPRT-amide derived from *Caenorhabditis elegans* thioredoxin reductase 2 (TRXR-2) sequence were conjugated to KLH and used to immunize rabbits (New England Peptides). After four immunizations, serum was collected and polyclonal antibodies were purified by affinity chromatography using a mix of the two peptides. For TRXR-2 immunoblotting, 100 worms from each strain (grown in OP50 for one generation) were manually collected at their first day of adulthood in 15 μL of lysis buffer (NaCl 150 m*M*, NP-40 1% and Tris-HCl 50 m*M* pH 8). After 3 cycles of freeze thawing in liquid nitrogen, 3 μL of Laemmli buffer 5× were added and the mix was heated at 95°C for 10 min. Proteins were separated by SDS-PAGE using a 10% polyacrylamide gel (BioRad) and transferred to Immobilon-P PVDF membranes (Millipore). Blots were probed with anti-TRXR-2 polyclonal antibody at a 1:1000 dilution and with rabbit anti-IgG (Sigma) at 1:10,000 as secondary antibody. The ECL kit (GE) was used for signal detection, following the manufacturer's instructions. Monoclonal anti-α-tubulin (Sigma) 1:10,000 was used as loading control. The quantification of TRXR-2 blots was performed using the ImageJ Software and the statistical analysis was performed with the Microsoft Excel Software.

References

1. An JH and Blackwell TK. SKN-1 links *C. elegans* mesendodermal specification to a conserved oxidative stress response. *Genes Dev* 17: 1882–1893, 2003.
2. Artal-Sanz M and Tavernarakis N. Prohibitin couples diapause signalling to mitochondrial metabolism during ageing in *C. elegans*. *Nature* 461: 793–797, 2009.
3. Calfon M, Zeng H, Urano F, Till JH, Hubbard SR, Harding HP, Clark SG, and Ron D. IRE1 couples endoplasmic reticulum load to secretory capacity by processing the XBP-1 mRNA. *Nature* 415: 92–96, 2002.
4. Damdimopoulos AE, Miranda-Vizuete A, Pelto-Huikko M, Gustafsson JA, and Spyrou G. Human mitochondrial thioredoxin. Involvement in mitochondrial membrane potential and cell death. *J Biol Chem* 277: 33249–33257, 2002.
5. de Castro E, Hegi de Castro S, and Johnson TE. Isolation of long-lived mutants in *Caenorhabditis elegans* using selection for resistance to juglone. *Free Radic Biol Med* 37: 139–145, 2004.
6. Doonan R, McElwee JJ, Matthijssens F, Walker GA, Houthoofd K, Back P, Matscheski A, Vanfleteren JR, and Gems D. Against the oxidative damage theory of aging: superoxide dismutases protect against oxidative stress but have little or no effect on life span in *Caenorhabditis elegans*. *Genes Dev* 22: 3236–3241, 2008.
7. Henderson ST and Johnson TE. daf-16 integrates developmental and environmental inputs to mediate aging in the nematode *Caenorhabditis elegans*. *Curr Biol* 11: 1975–1980, 2001.
8. Hendrick JP, Hodges PE, and Rosenberg LE. Survey of amino-terminal proteolytic cleavage sites in mitochondrial precursor proteins: leader peptides cleaved by two matrix proteases share a three-amino acid motif. *Proc Natl Acad Sci U S A* 86: 4056–4060, 1989.
9. Ishii N, Takahashi K, Tomita S, Keino T, Honda S, Yoshino K, and Suzuki K. A methyl viologen-sensitive mutant of the nematode *Caenorhabditis elegans*. *Mutat Res* 237: 165–171, 1990.
10. Johnston RJ and Hobert O. A microRNA controlling left/right neuronal asymmetry in *Caenorhabditis elegans*. *Nature* 426: 845–849, 2003.
11. Kimura KD, Tissenbaum HA, Liu Y, and Ruvkun G. daf-2, an insulin receptor-like gene that regulates longevity and diapause in *Caenorhabditis elegans*. *Science* 277: 942–946, 1997.
12. Labrousse AM, Zappaterra MD, Rube DA, and van der Bliek AM. *C. elegans* dynamin-related protein DRP-1 controls severing of the mitochondrial outer membrane. *Mol Cell* 4: 815–826, 1999.
13. Libina N, Berman JR, and Kenyon C. Tissue-specific activities of *C. elegans* DAF-16 in the regulation of lifespan. *Cell* 115: 489–502, 2003.
14. Lin K, Dorman JB, Rodan A, and Kenyon C. daf-16: An HNF-3/forkhead family member that can function to double the life-span of *Caenorhabditis elegans*. *Science* 278: 1319–1322, 1997.
15. Link CD. Expression of human beta-amyloid peptide in transgenic *Caenorhabditis elegans*. *Proc Natl Acad Sci U S A* 92: 9368–9372, 1995.
16. Link CD, Cypser JR, Johnson CJ, and Johnson TE. Direct observation of stress response in *Caenorhabditis elegans* using a reporter transgene. *Cell Stress Chaperones* 4: 235–242, 1999.
17. Link CD and Johnson CJ. Reporter transgenes for study of oxidant stress in *Caenorhabditis elegans*. *Methods Enzymol* 353: 497–505, 2002.
18. Link CD, Johnson CJ, Fonte V, Paupard M, Hall DH, Styren S, Mathis CA, and Klunk WE. Visualization of fibrillar amyloid deposits in living, transgenic *Caenorhabditis elegans* animals using the sensitive amyloid dye, X-34. *Neurobiol Aging* 22: 217–226, 2001.

19. Link CD, Silverman MA, Breen M, Watt KE, and Dames SA. Characterization of *Caenorhabditis elegans* lectin-binding mutants. *Genetics* 131: 867–881, 1992.
20. Link CD, Taft A, Kapulkin V, Duke K, Kim S, Fei Q, Wood DE, and Sahagan BG. Gene expression analysis in a transgenic *Caenorhabditis elegans* Alzheimer's disease model. *Neurobiol Aging* 24: 397–413, 2003.
21. Mello CC, Kramer JM, Stinchcomb D, and Ambros V. Efficient gene transfer in *C. elegans*: extrachromosomal maintenance and integration of transforming sequences. *EMBO J* 10: 3959–3970, 1991.
22. Miranda-Vizuete A, Fierro Gonzalez JC, Gahmon G, Burghoorn J, Navas P, and Swoboda P. Lifespan decrease in a *Caenorhabditis elegans* mutant lacking TRX-1, a thioredoxin expressed in ASJ sensory neurons. *FEBS Lett* 580: 484–490, 2006.
23. Olahova M, Taylor SR, Khazaipoul S, Wang J, Morgan BA, Matsumoto K, Blackwell TK, and Veal EA. A redox-sensitive peroxiredoxin that is important for longevity has tissue- and stress-specific roles in stress resistance. *Proc Natl Acad Sci U S A* 105: 19839–19844, 2008.
24. Ortiz CO, Etchberger JF, Posy SL, Frokjaer-Jensen C, Lockery S, Honig B, and Hobert O. Searching for neuronal left/right asymmetry: genomewide analysis of nematode receptor-type guanylyl cyclases. *Genetics* 173: 131–149, 2006.
25. Sijen T, Fleenor J, Simmer F, Thijssen KL, Parrish S, Timmons L, Plasterk RH, and Fire A. On the role of RNA amplification in dsRNA-triggered gene silencing. *Cell* 107: 465–476, 2001.
26. Thompson JD, Higgins DG, and Gibson TJ. CLUSTAL W: improving the sensitivity of progressive multiple sequence alignment through sequence weighting, position-specific gap penalties and weight matrix choice. *Nucleic Acids Res* 22: 4673–4680, 1994.
27. Wenick AS and Hobert O. Genomic cis-regulatory architecture and trans-acting regulators of a single interneuron-specific gene battery in *C. elegans*. *Dev Cell* 6: 757–770, 2004.
28. Wollman EE, d'Auriol L, Rimsky L, Shaw A, Jacquot JP, Wingfield P, Graber P, Dessarps F, Robin P, Galibert F, *et al.* Cloning and expression of a cDNA for human thioredoxin. *J Biol Chem* 263: 15506–15512, 1988.
29. Yoneda T, Benedetti C, Urano F, Clark SG, Harding HP, and Ron D. Compartment-specific perturbation of protein handling activates genes encoding mitochondrial chaperones. *J Cell Sci* 117: 4055–4066, 2004.